Available online at www.sciencedirect.com
SCIENCE DIRECT®
Journal of Solid State Chemistry 177 (2004) 4197–4204
JOURNAL OF SOLID STATE CHEMISTRY
www.elsevier.com/locate/jssc

Phase relation studies in the CeO_2–Gd_2O_3–ZrO_2 system

V. Grover, A.K. Tyagi*

Applied Chemistry Division, Bhabha Atomic Research Centre, Mumbai-400 085, India

Abstract

The phase relations in the CeO_2–Gd_2O_3–ZrO_2 system have been established after slowly cooling the samples from 1400 °C. Ceria has been used as a surrogate material in place of plutonia. About 80 compositions in $Zr_{1-x}Gd_xO_{2-x/2}$, $Ce_{1-x}Gd_xO_{2-x/2}$, $Ce_{1-x}Zr_xO_{2.00}$, $(Zr_{0.5}Ce_{0.5})_{1-x}Gd_xO_{2-x/2}$, $(Ce_{0.5}Gd_{0.5})_{1-x}Zr_xO_{1.75+x/4}$, $(Zr_{0.5}Gd_{0.5})_{1-x}Ce_xO_{1.75+x/4}$, and $(Ce_{0.8}Zr_{0.2})_xGd_{1-x}O_{1.5+x/2}$ were prepared by a three steps heating protocol. Based on the refinement of the XRD data, several phase regions namely; cubic fluorite type solid solution, *C*-type solid solution, and various biphasic regions could be delineated. This system showed the existence of a very wide cubic phase field. About 17.5 mol% $GdO_{1.5}$ was found to fully stabilize the cubic zirconia. On the other hand ceria did not stabilize the cubic zirconia. The anion-excess gadolinia, i.e., $Gd_{1-x}Ce_xO_{1.5+x}$ was found to retain the *C*-type lattite unlike pure gadolinia. The ternary phase relations were mainly characterized by the presence of wide homogeneity ranges of fluorite type or *C*-type phases.

Keywords: Solid state synthesis; Phase equilibria; Order–disorder; X-ray diffraction

1. Introduction

The development of uranium free inert matrix fuel is of worldwide interest as by using this concept it is possible to faster annihilate the large stock of plutonium and the realization of its energy value from the dismantled weapons and the accumulated stock from the nuclear power plants. Some of the potential materials, which can act as host lattice have been reviewed by Kleykamp [1]. In addition, this concept is also being contemplated to prepare targets for minor actinides transmutation using accelerators. In these fuels, an inert matrix serves as a support for the actinide phases. The inert matrix, as suggested by its name, does not lead to the formation of any fissile material, after the irradiation. Recently, we reported the sub-solidus phase equlibria in CeO_2–ThO_2–ZrO_2 under slow cooled conditions, which showed the presence of a limited cubic phase region [2]. A number of host lattices are being considered to act as an inert matrix, and their selection criteria, were also discussed therein.

In this manuscript we report the ternary phase relations in CeO_2–Gd_2O_3–ZrO_2 system which is highly relevant to the inert matrix fuel project. Ceria is used as a surrogate material [3,4] in place of plutonia. Gadolinia with its high neutron absorption cross section is a potential burnable poison and zirconia, being a highly stable material and with favorable neutronics is an ideal matrix. There are several reports on pseudo-binary phase diagrams/phase relations in system like Gd_2O_3–CeO_2 [5–8], CeO_2–ZrO_2 [9] and Gd_2O_3–ZrO_2 [10]. A considerable amount of work has been done on CeO_2–Gd_2O_3 system but mostly restricted to only ceria-rich phases (*F*-type cubic), from the point of view of ionic conductivity. Ceria doped with rare-earth oxides has been considered as one of the most promising materials for intermediate temperature solid oxide fuel cells because of their much higher ionic conductivity at lower temperatures in comparison with that of stabilized zirconia. Of all the RE_2O_3 dopants, Gd_2O_3 and Sm_2O_3-doped ceria was found to have the highest ionic conductivity [11,12].

*Corresponding author. Fax: +91-22-2550-5151.
E-mail address: aktyagi@magnum.barc.ernet.in (A.K. Tyagi).

0022-4596/$ - see front matter © 2004 Elsevier Inc. All rights reserved.
doi:10.1016/j.jssc.2004.07.052

Brauer et al. [5] reported the cubic lattice parameter in $Ce_{1-x}Gd_xO_{2-x/2}$ ($x=0.1$–0.3) system way back in 1954. The $Ce_{1-x}Gd_xO_{2-x/2}$ system was also studied by Bevan and Summerville [6] after quenching from 1600 °C where they found a biphasic region consisting of *F*- and *C*-type solid solutions separating monophasic *F*- and *C*-type solid solutions on either side of $F+C$ region. In addition, they had observed another biphasic field containing *B*- (monoclinic) and *C*-type phases in highly Gd_2O_3-rich region though earlier studies on this systems by Brauer and Gradinger [5] have shown a continuous range of solid solutions in this series without any biphasic region. Tianshu et al. [7] also reported the *F*-type phases in $Ce_{1-x}Gd_xO_{2-x/2}$ ($0.05\leqslant x\leqslant 0.4$). Heggestad et al. [8] studied the system $Ce_{1-x}Gd_xO_{2-x/2}$ ($x=0.1$–0.9) to reveal the presence of *F*-type phase upto $x=0.4$ and a bcc phase there after. The system was recently studied by us also over the entire range (i.e. $Ce_{1-x}Gd_xO_{2-x/2}$; $x=0.05$–0.95). It was observed that an *F*-type cubic solid solution exists upto $x=0.4$ which gradually changes to *C*-type solid solution without showing any miscibility gap or the biphasic region [13].

The phase diagram of CeO_2–ZrO_2 system consist of two regions namely monoclinic solid solution up to about 18 mol% of ceria in zirconia and two-phase region consisting of tetragonal solid solution and cubic ceria-rich solid solution. On heating to appropriately higher temperatures, depending upon the composition, the monoclinic and tetragonal solid solutions were shown to become tetragonal and cubic solid solution, respectively [9].

Some studies have also been reported on Gd_2O_3–ZrO_2 system. Wang et al. [14] have studied the phase relation in $Gd_xZr_{1-x}O_{2-x/2}$ system ($0.16\leqslant x\leqslant 0.62$) and found that a defect fluorite lattice exists for $0.18\leqslant x\leqslant 0.45$ and $0.55\leqslant x\leqslant 0.62$ whereas a pyrochlore type compound exists for $0.45\leqslant x\leqslant 0.55$. Gd_2O_3–ZrO_2 system has also been studied by Feighery et al. [15]. They observed the existence of several phases like single phasic t-ZrO_2, a two phase mixture of t-ZrO_2 and a defect cubic fluorite phase, single phasic defect fluorite, pyrochlore, *C*-type Gd_2O_3 and m-Gd_2O_3 with increasing concentration of Gd_2O_3. Furthermore it has been found that pyrochlore gadolinium zirconate, $Gd_2Zr_2O_7$, is very promising for immobilization of plutonium compared to the corresponding titanate $Gd_2Ti_2O_7$ currently being considered for Pu disposal [16–19].

In order to identify still newer inert matrices, it is required to construct the phase relations in the desired systems so as to prepare suitable single phasic compositions. It may be added here that the ternary phase diagrams on nuclear materials are scantily reported compared to the pseudo-binary phase diagrams. Schleifer et al. [20] reported the phase equilibria in UO_2–ZrO_2–Ln_2O_3 (Ln = lanthanides) in the temperature range 1270–1670 K. In this manuscript, the sub-solidus phase relations in CeO_2–Gd_2O_3–ZrO_2, under slow cooled conditions is being reported for the first time.

2. Experimental

CeO_2, ZrO_2 and Gd_2O_3 (all 99.9%) were used as the starting materials, which were heated at 900 °C for overnight prior to the further use. These starting materials were well characterized by powder XRD before use. About 80 compositions in CeO_2–Gd_2O_3–ZrO_2 system were prepared by a three stage heating protocol, as follows: The intimately ground mixtures were heated in the pellet form at 1200 °C for 36 h, followed by second heating at 1300 °C for 36 h after regrinding and repelletizing. In order to attain a better homogeneity, the products obtained after second heating were again reground, pelletized and heated at 1400 °C for 48 h, which was the final annealing temperature of all the specimens. The heating and cooling rates were 2 °C/min in all the annealing steps and the atmosphere was static air. The XRD patterns were recorded from 10° to 90°on a Philips X-ray diffractometer (Model PW 1710) with monochromatized Cu-$K\alpha$ radiation ($K\alpha_1=1.5406$ Å and $K\alpha_2=1.5444$ Å). Silicon was used as an external standard for calibration of the instrument. The XRD patterns were well analyzed by comparing with the reported ones. In order to determine the solubility limits, the lattice parameters were refined by a software (POWDERX) based on least-squares method.[1]

3. Results and discussion

3.1. $Zr_{1-x}Gd_xO_{2-x/2}$ system

Table 1 gives the details of the phases and their lattice parameters obtained by refinement of the XRD data. Typical XRD patterns for this series are given in Fig. 1. Powder XRD pattern revealed that the ZrO_2 used in the present investigation was monoclinic and Gd_2O_3 was cubic (*C*-type). In order to make a better comparison all the three reactants were also heated at 1400 °C for 48 h under identical conditions. It was found that after this heat treatment *C*-type gadolinia got irreversibly transformed to *B*-type (monoclinic) even despite slow cooling. This observation would be explained later. The first nominal composition in this series, i.e., $Zr_{0.95}Gd_{0.05}O_{1.975}$ was found to be biphasic consisting of tetragonal phase and the monoclinic phase (Table 1). The next two compositions, i.e., $Zr_{0.90}Gd_{0.10}O_{1.95}$ and $Zr_{0.85}Gd_{0.15}O_{1.925}$

[1] V.S. Jakkal, BARC, Mumbai, Powderx: a FORTRAN software for refining the unit cell parameter for the powder diffraction pattern, private communication.

Table 1
Phase analysis and lattice parameters of the phases in $Zr_{1-x}Gd_xO_{2-x/2}$ system

S. no	Nominal composition	Phase analysis	a (Å)	Volume (Å^3)
1	ZrO_2	M a	5.313(1)	140.7(1)
		b	5.212(1)	
		c	5.147(1)	
		β	99.22^0	
2	$Zr_{0.95}Gd_{0.05}O_{1.975}$		$a_m = 5.33(2), b_m = 5.19(2),$	[a]
		M	$c_m = 5.17(1), \beta = 99.3(4)$	$V_m = 141.0(9)$
		T	$a_T = 5.121(6); c_T = 5.25(4)$	$V_T = 137.5(4)$
3	$Zr_{0.90}Gd_{0.10}O_{1.95}$	M	[a]	[a]
		F	5.166(2)	137.83(8)
4	$Zr_{0.85}Gd_{0.15}O_{1.925}$	M	[a]	[a]
		F	5.165(1)	137.82(5)
5	$Zr_{0.80}Gd_{0.20}O_{1.90}$	F	5.1714(1)	138.30(5)
6	$Zr_{0.70}Gd_{0.30}O_{1.85}$	F	5.199(2)	140.49(9)
7	$Zr_{0.60}Gd_{0.40}O_{1.80}$	F	5.241(2)	143.9(1)
8	$Zr_{0.50}Gd_{0.50}O_{1.75}$	P	10.541(3)	1171.5(7)
9	$Zr_{0.40}Gd_{0.60}O_{1.70}$	P[b]	5.309(3)	149.6(1)
10	$Zr_{0.30}Gd_{0.70}O_{1.65}$	C	[a]	[a]
		P[b]	5.326(2)	151.11(9)
11	$Zr_{0.20}Gd_{0.80}O_{1.60}$	C	10.752(3)	1242.9(6)
		P[b]	5.317(2)	150.31(8)
12	$Zr_{0.10}Gd_{0.90}O_{1.55}$	C	10.782(4)	1253.5(8)
		P[b]	[a]	[a]
13	$Zr_{0.05}Gd_{0.95}O_{1.525}$	M'	[a]	[a]
		C	10.799(6)	1259(1)
14	$Zr_{0.025}Gd_{0.975}O_{1.512}$	M'		
		C	10.796(2)	1258.3(3)

M: monoclinic ZrO_2 type; M': monoclinic Gd_2O_3 type; F = fluorite ; P = pyrochlore; C: C-type; a_m, b_m, c_m, V_m, β = lattice parameters and volume of monoclinic phase. T: teragonal phase; a_T, c_T, V_T: lattice parameters and volume of tetragonal phase.
[a]Not refined due to insignificant intensity.
[b]Refined on fluorite type basis cell.

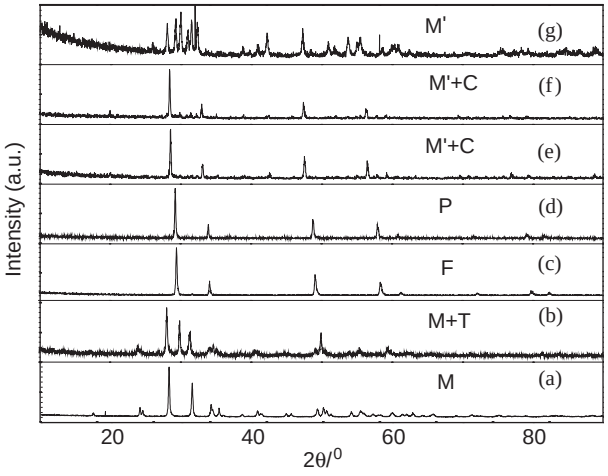

Fig. 1. XRD patterns of: (a) ZrO_2; (b) $Gd_{0.05}Zr_{0.95}O_{1.975}$; (c) $Gd_{0.40}Zr_{0.60}O_{1.80}$; (d) $Gd_{0.50}Zr_{0.50}O_{1.75}$; (e) $Gd_{0.95}Zr_{0.05}O_{1.525}$; (f) $Gd_{0.975}Zr_{0.025}O_{1.512}$; (g) Gd_2O_3.

were biphasic with a fluorite-type phase and a monoclinic phase but with a concomitant reduction in the peak intensity of monoclinic zirconia. The next composition $Zr_{0.80}Gd_{0.20}O_{1.90}$ was found to be fully stabilized zirconia. Therefore, it can be inferred that about 17.5 mol% $GdO_{1.5}$, i.e., the average between $Zr_{0.85}Gd_{0.15}O_{1.925}$ (biphasic) and $Zr_{0.80}Gd_{0.20}O_{1.90}$ (monophasic) can fully stabilize the cubic zirconia under the experimental conditions employed by us. The stabilized zirconia exists up to the nominal composition $Zr_{0.60}Gd_{0.40}O_{1.80}$. There is an increase in lattice parameter of the fluorite-type phase, i.e., the stabilized zirconia, from 5.166(2) to 5.241(2) Å on going from $Zr_{0.90}Gd_{0.10}O_{1.95}$ to $Zr_{0.60}Gd_{0.40}O_{1.80}$, thereby indicating the presence of a wide homogeneity range of gadolinia-stabilized-zirconia. The composition $Zr_{0.50}Gd_{0.50}O_{1.75}$ was found to be a pyrochlore phase, which existed till the composition $Zr_{0.40}Gd_{0.60}O_{1.70}$. The peaks due to C-type gadolinia started appearing after the composition $Zr_{0.30}Gd_{0.70}O_{1.65}$. Though gadolinia (which is C type at ambient temperature) when heated to 1400 °C and then slow cooled to room temperature, it's monoclinic modification (B-type) is stabilized as revealed by its XRD pattern. Doping of ZrO_2 in gadolinia stabilizes the C-type modification even after heating to 1400 °C. This can be explained based on the structure and phase diagram of rare-earth sesquioxides as a function of temperature as well as ionic size [21]. At temperatures below 2000 °C three types of polymorphs,

designated as A (hexagonal), B (monoclinic) and C (cubic) have been reported in RE_2O_3 (RE = rare-earths) depending upon the rare-earth ionic size, e.g., the A-type RE_2O_3 exists for RE = La–Nd. In general on going from La to Lu, the structure of RE_2O_3 changes from A- to B-type and finally to C-type. Gd_2O_3, i.e., one of the end members of present investigation exists in C-type modification at ambient temperature and is known to undergo a phase transition to monoclinic modification, i.e., the B-type at about 1200 °C. Foex et al. [22] have reported that the stability of C-type modification increases on decreasing the RE^{3+} ionic size. In fact, Lu_2O_3, which is C-type, directly melts without undergoing any phase transition. It is obvious that the average ionic size at the Gd^{3+} site decreases on incorporation of Zr^{4+}, which explains the additional stability of the C-type modification of Gd_2O_3 on Zr^{4+} incorporation. However, the role of additional oxygens associated with substitution of Gd^{3+} by Zr^{4+}, is not known at this stage. The similar observations in CeO_2–Gd_2O_3 system have been reported in details elsewhere [13,23]. Recently, we reported structural analysis of anion-rich Gd_2O_3, i.e., $Gd_{1-x}Ce_xO_{1.5+x/2}$ ($x = 0.20$ and 0.40). These are isostructural with C-type rare earth oxides, with excess anions required for charge balance. They have body centered cubic lattice (space group Ia-3, No. 206, $Z = 32$). The structural analysis reveals that there are two different kinds of metal ion sites, namely 8b and 24d and two different kinds of anion sites namely 48e and 16c. The excess anions occupy 16c site [23]. The highly gadolinia rich phases like $Zr_{0.05}Gd_{0.95}O_{1.525}$ and $Zr_{0.025}Gd_{0.975}O_{1.512}$, etc. showed the presence of B-type phase also (monoclinic Gd_2O_3) in addition to C-type phase (cubic gadolinia) and thereby indicating that 2.5 or 5 mol% zirconia is not sufficient to fully stabilize C-type gadolinia. A striking difference between ZrO_2–Gd_2O_3 and CeO_2–Gd_2O_3 systems is that in the case of latter several single phasic C-type compositions could be obtained contrary to the ZrO_2–Gd_2O_3 system in which C-type phase was always coexisting with pyrochlore phase. One reason of coexistence of C-type phase with pyrochlore phase could be the exceptional stability of $Gd_2Zr_2O_7$ pyrochlore phase. The CeO_2–Gd_2O_3 system does not show the formation of any pyrochlore phase [13] and on going from CeO_2 to Gd_2O_3 end, there is a gradual change over of the modification from F- to C-type lattice in $Ce_{1-x}Gd_xO_{2-x/2}$ series.

3.2. $Ce_{1-x}Gd_xO_{2-x/2}$ system

As mentioned earlier, this system is characterized by the presence of only two phase fields namely F-type cubic phase from CeO_2 to $Ce_{0.60}Gd_{0.40}O_{1.80}$ and C-type cubic from $Ce_{0.50}Gd_{0.50}O_{1.75}$ to $Ce_{0.05}Gd_{0.95}O_{1.525}$ (Table 2). Detailed phase analyses in this system has been recently reported elsewhere [13]. The lattice parameter of F-type solid solutions increases on incorporation of Gd^{3+}. The ionic radii of Gd^{3+} and Ce^{4+}, in 8-fold coordination, are 0.97 and 0.90 Å, respectively [24]. Therefore, based on the relative ionic size considerations, one can explain the increase in the cubic lattice parameter of fluorite-type phases on incorporation of Gd^{3+} ion at the Ce^{4+} sites. Likewise, one would expect a decrease in lattice parameters of C-type Gd_2O_3 on Ce^{4+} incorporation. However, the lattice parameter of gadolinia shows a progressive increase on incorporation of Ce^{4+}. This unusual observation can be attributed to the ionic repulsion between excess interstitial anions, required for charge neutralization, which probably causes dilation of the unit cell. A similar unusual trend was observed by us in fluoride systems also, e.g., CaF_2–YF_3 system [25].

Table 2
Phase analysis and lattice parameters of the phases in $Ce_{1-x}Gd_xO_{2-x/2}$ system

S. no.	Nominal composition	Phase analyses	a (Å)	Volume (Å^3)
1	CeO_2	F	5.411(1)	158.4(1)
2	$Ce_{0.90}Gd_{0.10}O_{1.95}$	F	5.410(1)	158.32(7)
3	$Ce_{0.85}Gd_{0.15}O_{1.925}$	F	5.425(1)	159.67(5)
4	$Ce_{0.80}Gd_{0.20}O_{1.90}$	F	5.432(1)	160.3(1)
5	$Ce_{0.70}Gd_{0.30}O_{1.85}$	F	5.437(2)	160.7(1)
6	$Ce_{0.60}Gd_{0.40}O_{1.80}$	F	5.439(2)	160.9(1)
7	$Ce_{0.50}Gd_{0.50}O_{1.75}$	C	10.862(2)	1281.5(4)
8	$Ce_{0.40}Gd_{0.60}O_{1.70}$	C	10.854(3)	1277.5(6)
9	$Ce_{0.30}Gd_{0.70}O_{1.65}$	C	10.855(1)	1279.1(3)
10	$Ce_{0.20}Gd_{0.80}O_{1.60}$	C	10.849(1)	1276.5(3)
11	$Ce_{0.15}Gd_{0.85}O_{1.575}$	C	10.838(1)	1273.2(2)
12	$Ce_{0.10}Gd_{0.90}O_{1.55}$	C	10.837(1)	1273.0(9)
13	$Ce_{0.05}Gd_{0.95}O_{1.525}$	C	10.831(1)	1271.4(3)
14	Gd_2O_3	C[a]	10.813(1)	1264.3(1)

C: C-type solid solution; F: fluorite-type solid solution.
[a]Prior to the heat treatment.

3.3. $Ce_{1-x}Zr_xO_{2.00}$ system

The phase relation studies in this binary system, under identical conditions, have been earlier reported as a part of ThO_2–CeO_2–ZrO_2 ternary phase relation [2]. A few salient features observed are as follows: about 20 mol% of ZrO_2 is soluble in the lattice of ceria while maintaining single-phase. The lattice parameter of the cubic phase further decreases up to the composition $Ce_{0.60}Zr_{0.40}O_2$, but an additional phase also appears in compositions beyond $Ce_{0.80}Zr_{0.20}O_2$. This observation indicates that the solubility of zirconia in ceria is slightly higher than 20 mol%. A nearly single-phase tetragonal zirconia type modification was obtained at the nominal composition $Ce_{0.20}Zr_{0.80}O_2$, which is in a reasonably good agreement with an earlier report [26] in which a single-phase tetragonal zirconia was obtained at the nominal composition $Ce_{0.16}Zr_{0.84}O_2$. An important

observation of this system is the absence of the cubic zirconia phase. Thus probably instead of isovalent substitution, one needs substitution by a suitable aliovalent ion, ca. Y^{3+} or Ca^{2+}, which leads to oxygen vacancies in the anionic sub-lattice, to stabilize the cubic zirconia. Thus the zirconia in cubic modification is stabilized due to two factors namely, an increase in average cationic size and increase in entropy contribution in free energy on aliovalent ion substitution.

3.4. $(Zr_{0.5}Ce_{0.5})_{1-x}Gd_xO_{2-x/2}$ system

Table 3 gives the details of the phases obtained in the $(Zr_{0.5}Ce_{0.5})_{1-x}Gd_xO_{2-x/2}$ system. The trend in XRD patterns of the nominal compositions in the $(Zr_{0.5}Ce_{0.5})_{1-x}Gd_xO_{2-x/2}$ system is shown in Fig. 2. One of the end members of this series, i.e., the nominal composition $Zr_{0.5}Ce_{0.5}O_2$ is itself biphasic, consisting of cubic and tetragonal phases, i.e., zirconia-doped ceria (cubic phase) and ceria-stabilized tetragonal zirconia. From XRD analysis, it was found that even addition of 10 mol% $GdO_{1.5}$ into $Zr_{0.5}Ce_{0.5}O_2$, i.e., to give nominal composition $Zr_{0.45}Ce_{0.45}Gd_{0.10}O_{1.95}$, results in the formation of a monophasic product with typical fluorite type XRD pattern. This trend continues till $Zr_{0.40}Ce_{0.40}Gd_{0.20}O_{1.90}$. The observation of a monophasic defective fluorite type phase for these compositions can be explained based on the fact that gadolinia is stabilizing zirconia and which in turn forms a solid solution with ceria. The XRD patterns of next four compositions, i.e., $Zr_{0.35}Ce_{0.35}Gd_{0.30}O_{1.85}$ to $Zr_{0.20}Ce_{0.20}Gd_{0.60}O_{1.80}$ were found to have somewhat broad peaks, which signifies the occurrence of a phase separation of

Table 3
Phase analysis and lattice parameters of the phases in $(Ce_{0.5}Zr_{0.5})_{1-x}Gd_xO_{2-x/2}$ system

S. no.	Nominal composition	Phase analysis	a (Å)	Volume (Å^3)
1	$Ce_{0.5}Zr_{0.5}Gd_{0.00}O_2$	F	5.344(1)	152.6(1)
		T a_T	5.141(5)	138.8(3)
		T C_T	5.254(8)	
2	$Ce_{0.45}Zr_{0.45}Gd_{0.10}O_{1.95}$	F	5.2852(7)	147.63(3)
4	$Ce_{0.40}Zr_{0.40}Gd_{0.20}O_{1.90}$	F	5.294(1)	148.33(6)
5	$Ce_{0.35}Zr_{0.35}Gd_{0.30}O_{1.85}$	F[a]	5.324(2)	150.89(9)
6	$Ce_{0.30}Zr_{0.30}Gd_{0.40}O_{1.80}$	F[a]	5.352(1)	153.27(5)
7	$Ce_{0.25}Zr_{0.25}Gd_{0.50}O_{1.75}$	F[a]	5.368(2)	154.65(10)
8	$Ce_{0.20}Zr_{0.20}Gd_{0.60}O_{1.70}$	F[a]	5.377(1)	155.44(6)
9	$Ce_{0.15}Zr_{0.15}Gd_{0.70}O_{1.65}$	C	10.77(1)[b]	1250(2)[b]
		F		
10	$Ce_{0.10}Zr_{0.10}Gd_{0.80}O_{1.60}$	C	10.799(7)[b]	1259(1)[b]
		F		
11	$Ce_{0.05}Zr_{0.05}Gd_{0.90}O_{1.55}$	C	10.806(3)	1261.8(6)

C: C-type solid solution; F: fluorite-type solid solution; T: tetragonal.
[a]Broad peaks were observed signifying the presence of another unidentified phase.
[b]Not refined due to insignificant intensity.

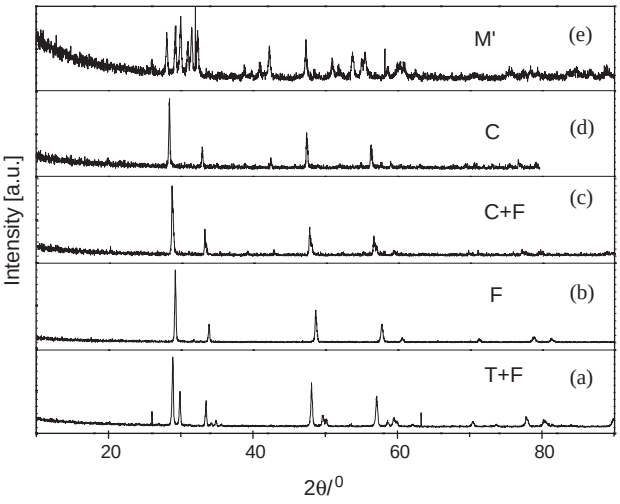

Fig. 2. XRD patterns of: (a) $Zr_{0.50}Ce_{0.50}O_{2.00}$; (b) $Zr_{0.40}Ce_{0.40}Gd_{0.20}O_{1.95}$; (c) $Zr_{0.15}Ce_{0.15}Gd_{0.70}O_{1.65}$; (d) $Zr_{0.05}Ce_{0.05}Gd_{0.90}O_{1.55}$; (e) Gd_2O_3.

these compositions into two phases with close by cell parameters. It appears that these two products consists of anion-deficient fluorite-type, i.e., $(CeZr)_{1-x}Gd_xO_{2-x/2}$ and anion-excess C-type gadolinia lattice, i.e., $Gd_{1-x}(ZrCe)_xO_{1.5+x/2}$. It is difficult to assign the exact compositions to these two lattices by XRD data alone. The presence of C-type phase in these compositions can be ascertained by the presence of C-type superstructure peaks in $Zr_{0.15}Ce_{0.15}Gd_{0.70}O_{1.65}$ at $2\theta = 35.200°$, 39.335°, 42.690°, etc. in addition to F-type peaks. Single phasic C-type cubic phase was obtained at $Zr_{0.05}Ce_{0.05}Gd_{0.90}O_{1.55}$. The structure of this material can be explained based on the anion-rich C-type gadolinia lattice. As is evident from Table 3, the lattice parameter of the F-type solid solution increases systematically with increase in $GdO_{1.5}$ content which is due to the increase in average cationic size with the substitution of Gd^{3+} in place of Zr^{4+} and Ce^{4+}. For the same reason the lattice parameter of the C-type solid solution also increases with increasing the $GdO_{1.5}$ content.

3.5. $(Ce_{0.5}Gd_{0.5})_{1-x}Zr_xO_{1.75+x/4}$

Table 4 describes various phases and their lattice parameters observed in this series. The typical XRD patterns of this series are shown in Fig. 3. One of the end members of this series ($Ce_{0.5}Gd_{0.5}O_{1.75}$) was found to be a C-type cubic ceria-gadolinia solid solution [13]. However, the next nominal composition, $Ce_{0.45}Gd_{0.45}Zr_{0.10}O_{1.775}$ was found to be an F-type cubic phase. The conversion of C-type cubic phase $Ce_{0.5}Gd_{0.5}O_{1.75}$ in to an F-type phase on incorporation of 10 mol% ZrO_2 can be attributed to incorporation of excess anions accompanied by Zr^{4+} substitution. It may be noted that the C-type $GdO_{1.5}$ is obtained due to ordering of 0.5

Table 4
Phase analysis and lattice parameters of the products in $(Ce_{0.5}Gd_{0.5})_{1-x}Zr_xO_{1.75+x/4}$ system

S. no.	Nominal composition	Phase analysis	a (Å)	Volume (Å^3)
1	$Ce_{0.5}Gd_{0.5}Zr_{0.00}O_{1.75}$	C	10.862(2)	1281.5(1)
2	$Ce_{0.45}Gd_{0.45}Zr_{0.10}O_{1.775}$	F	5.422(1)	159.36(7)
3	$Ce_{0.40}Gd_{0.40}Zr_{0.20}O_{1.80}$	F[a]	5.397(2)	157.23(10)
4	$Ce_{0.35}Gd_{0.35}Zr_{0.30}O_{1.825}$	F[a]	5.357(3)	153.7(1)
5	$Ce_{0.30}Gd_{0.30}Zr_{0.40}O_{1.85}$	F[a]	5.310(2)	149.72(9)
6	$Ce_{0.25}Gd_{0.25}Zr_{0.50}O_{1.875}$	F	5.267(2)	146.10(8)
7	$Ce_{0.20}Gd_{0.20}Zr_{0.60}O_{1.90}$	F	5.234(1)	143.40(6)
8	$Ce_{0.15}Gd_{0.15}Zr_{0.70}O_{1.925}$	F	5.212(2)	141.57(9)
9	$Ce_{0.10}Gd_{0.10}Zr_{0.80}O_{1.95}$	F	5.191(1)	138.9(6)
		M	[b]	[b]
10	$Ce_{0.05}Gd_{0.05}Zr_{0.90}O_{1.975}$	F	5.174(8)	138.5(4)
		M	[b]	[b]

C: C-type solid solution; F: fluorite-type solid solution; M: monoclinic zirconia.
[a]Board peaks signifying the presence of another unidentified phase.
[b]Not refined due to insignificant intensity.

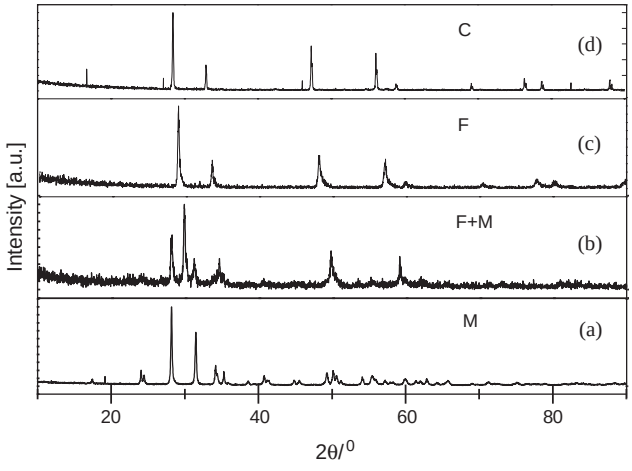

Fig. 3. XRD Patterns of: (a) ZrO_2; (b) $Gd_{0.05}Ce_{0.05}Zr_{0.90}O_{1.975}$; (c) $Gd_{0.40}Ce_{0.40}Zr_{0.20}O_{1.80}$; (d) $Gd_{0.50}Ce_{0.50}O_{1.75}$.

vacancies in fluorite-type basis cell of $GdO_{1.5}$. The substitution of tetravalent cations such as Ce^{4+} and Zr^{4+} at Gd^{3+} site fills the anion-vacancies, which after a certain threshold, up to which C-type lattice is maintained, leads to the formation of solid solution with a defective fluorite-type unit cell in which all the three cations, Gd^{3+}, Zr^{4+} and Ce^{4+}, are statistically distributed. XRD patterns of subsequent compositions, i.e., $Ce_{0.40}Gd_{0.40}Zr_{0.20}O_{1.80}$ to $Ce_{0.30}Gd_{0.30}Zr_{0.40}O_{1.85}$ showed the presence of broad peaks, which again signifies the occurrence of a phase separation in these three compositions into two phases with somewhat close-by lattice parameters. One of these two phases is fluorite-type phase with a wide homogeneity range as there is a systematic decrease in the lattice parameter on incorporating more and more of smaller ion Zr^{4+}. After these compositions, a monophasic fluorite type phase was obtained corresponding to the nominal compositions $Ce_{0.25}Gd_{0.25}Zr_{0.50}O_{1.825}$ to $Ce_{0.15}Gd_{0.15}Zr_{0.70}O_{1.825}$ with a unit cell parameters decreasing from 5.267 to 5.212 Å, which is nothing but an anion-deficient defective fluorite type lattice, due to the presence of 15 mol% $GdO_{1.5}$. Further zirconia rich compositions (with 80 and 90 mol% ZrO_2) were found to contain monoclinic ZrO_2 also, in addition to fluorite-type phase. It can be clearly seen from Table 4 that the lattice parameter for the F-type solid solution systematically decreases on incorporating 10 mol% ZrO_2 to 90 mol% ZrO_2 from 5.422(1) to 5.16(2) Å. This can be explained on the basis of decrease in average cationic radius on doping Zr^{4+} in place of Ce^{4+} and Gd^{3+}. This shows that fluorite type phase in $(Ce_{0.5}Gd_{0.5})_{1-x}Zr_xO_{1.75+x/4}$ series has got a wide homogeneity range.

3.6. $(Zr_{0.5}Gd_{0.5})_{1-x}Ce_xO_{1.75+x/4}$ system

Typical XRD patterns belonging to this series are given in Fig. 4. Various phases and the corresponding lattice parameters observed in this series are listed in Table 5. One of the end members of this series ($Zr_{0.5}Gd_{0.5}O_{1.75}$) was a pyrochlore, characterized by the presence of a few weak superstructure peaks at $2\theta = 14.5°$, 28.17°, 37.2°, 44.7° and 51.3°, with lattice parameter 10.542 Å (Table 5). The observation of pyrochlore phase for this composition could be rationalized based on the fact that the final calcination temperature was 1400 °C, which is much below the order–disorder transition temperature at which $Zr_2Gd_2O_7$ becomes defect fluorite (>1573° C), and also because of the slow cooling rate used during the synthesis. Surprisingly, these weak peaks disappear

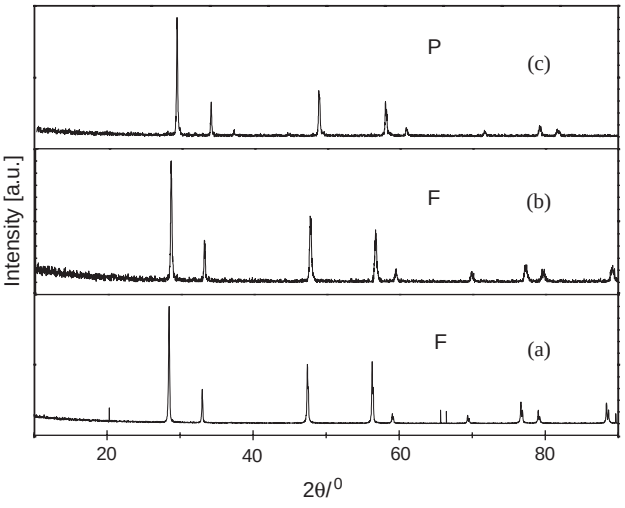

Fig. 4. XRD patterns of: (a) CeO_2; (b) $Gd_{0.15}Zr_{0.15}Ce_{0.70}O_{1.925}$; (c) $Gd_{0.50}Zr_{0.50}O_{1.75}$.

Table 5
Phase analysis and lattice parameters of the products in $(Zr_{0.5}Gd_{0.5})_{1-x}Ce_xO_{1.75+x/4}$ system

S. no.	Nominal composition	Phase analysis	a (Å)	Volume (Å^3)
1	$Zr_{0.5}Gd_{0.5}Ce_{0.00}O_{1.75}$	P	10.541(3)	1171.5(7)
2	$Zr_{0.45}Gd_{0.45}Ce_{0.10}O_{1.775}$	F[a]	5.306(6)	149.4(3)
3	$Zr_{0.40}Gd_{0.40}Ce_{0.20}O_{1.80}$	F[a]	5.307(2)	149.5(1)
4	$Zr_{0.35}Gd_{0.35}Ce_{0.30}O_{1.825}$	F[a]	5.332(2)	151.59(9)
5	$Zr_{0.30}Gd_{0.30}Ce_{0.40}O_{1.85}$	F[a]	5.356(3)	153.6(2)
6	$Zr_{0.25}Gd_{0.25}Ce_{0.50}O_{1.875}$	F[a]	5.368(2)	154.69(10)
7	$Zr_{0.20}Gd_{0.20}Ce_{0.60}O_{1.90}$	F[a]	5.371(2)	154.97(9)
8	$Zr_{0.15}Gd_{0.15}Ce_{0.70}O_{1.925}$	F	5.373(1)	155.14(6)
9	$Zr_{0.10}Gd_{0.10}Ce_{0.80}O_{1.95}$	F	5.3849(2)	156.15(1)
10	$Zr_{0.05}Gd_{0.05}Ce_{0.90}O_{1.975}$	F	5.395(3)	157.0(2)
11	CeO_2	F	5.4111(1)	158.4(1)

P: pyrochlore; F: fluorite-type solid solution.
[a]Broad peaks signifying the presence of another unidentified phase.

Table 6
Phase analysis and room temperature lattice parameters of the phases in $(Ce_{0.8}Zr_{0.2})_{1-x}Gd_xO_{2-x/2}$ system, annealed at 1400 °C (in air) followed by slow cooling.

S. no.	Nominal composition	Phase analysis	a (Å)	Volume (Å^3)
1	$Ce_{0.8}Zr_{0.2}Gd_{0.00}O_2$	F	5.356(1)	153.6(1)
2	$Ce_{0.72}Zr_{0.18}Gd_{0.10}O_{1.95}$	F	5.3617(5)	154.14(2)
4	$Ce_{0.64}Zr_{0.16}Gd_{0.20}O_{1.90}$	F	5.388(1)	156.46(5)
5	$Ce_{0.56}Zr_{0.14}Gd_{0.30}O_{1.85}$	F	5.410(2)	158.3(1)
6	$Ce_{0.48}Zr_{0.12}Gd_{0.40}O_{1.80}$	F	5.4133(9)	158.63(5)
7	$Ce_{0.40}Zr_{0.10}Gd_{0.50}O_{1.75}$	F	5.4139(7)	158.69(3)
8	$Ce_{0.32}Zr_{0.08}Gd_{0.60}O_{1.70}$	C	10.86(2)	1279(3)
9	$Ce_{0.24}Zr_{0.06}Gd_{0.70}O_{1.65}$	C	10.840(4)	1273.7(9)
10	$Ce_{0.16}Zr_{0.04}Gd_{0.80}O_{1.60}$	C	10.823(1)	1267.9(3)
11	$Ce_{0.08}Zr_{0.02}Gd_{0.90}O_{1.55}$	C	10.822(1)	1267.3(2)

C: C-type solid solution; F: fluorite-type solid solution.

even by 10 mol% doping of CeO_2 in $Zr_2Gd_2O_7$ lattice. These few compositions ($(Zr_{0.5}Gd_{0.5})_{1-x}Ce_xO_{1.75+x/4}$; $x=0.1$–0.6) were found to have broad peaks in their XRD patterns, which showed the presence of an F-type lattice with another unidentified lattice, presumably another F-type lattice. The refinement of the XRD data for the major fluorite phase gave the lattice parameters which increase with increase in ceria content which can be explained on the basis of increase in average cationic radius on doping ceria. The observation of fluorite type phase for these compositions can be attributed to the fact that Ce^{4+} prefers 8-fold coordination in oxides, by and large, whereas preference for the octahedral coordination by the B site cation is the prerequisite for pyrochlore formation. The average cationic size at Zr^{4+} site increases by Ce^{4+} substitution, which is not favorable for the formation of pyrochlore phase. The compositions $Zr_{0.2}Gd_{0.20}Ce_{0.70}O_{1.90}$–$Zr_{0.05}Gd_{0.05}Ce_{0.90}O_{1.975}$ were found to be single phasic F-type with an upward trend in lattice parameter, which could be attributed based on the increase in average cationic size in these compositions.

3.7. $(Ce_{0.8}Zr_{0.2})_xGd_{1-x}O_{1.5+x/2}$ series

Table 6 shows the phase analysis and lattice parameters for the phases obtained in this series. The typical XRD patterns of this series are shown in Fig. 5. One of the end members, Gd_2O_3, which is a C-type to begin but becomes monoclinic after heating at 1400 °C for 48 h. Surprisingly, on doping it with 10 mol% of $Ce_{0.8}Zr_{0.2}O_2$, which itself is F-type cubic, it retains C-type lattice. This observation can be explained on the basis of reduction in average cationic size thus stabilizing C-type modification. This trend continues in 20 mol% of $Ce_{0.8}Zr_{0.2}O_2$ in $GdO_{1.5}$ which is again clearly a C-type solid solution. The C-type phase exists

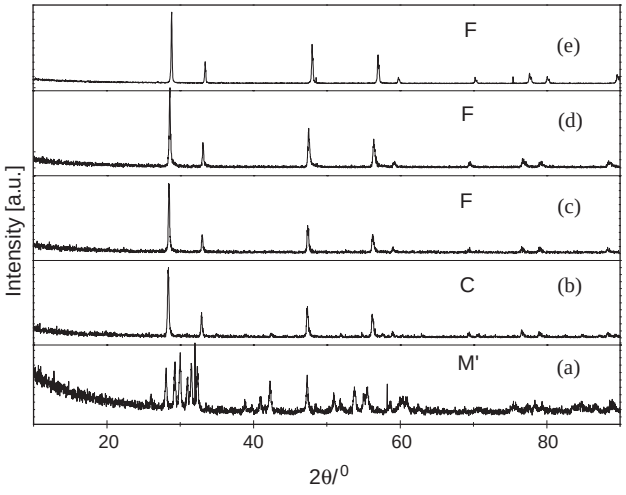

Fig. 5. XRD patterns of: (a) Gd_2O_3; (b) $Gd_{0.70}Ce_{0.24}Zr_{0.06}O_{1.65}$; (c) $Gd_{0.50}Ce_{0.40}Zr_{0.10}O_{1.75}$; (d) $Gd_{0.30}Ce_{0.56}Zr_{0.14}O_{1.85}$; (e) $Ce_{0.80}Zr_{0.20}O_{2.00}$.

till 40 mol% $Ce_{0.8}Zr_{0.2}O_2$ in $GdO_{1.5}$ but with the gradual reduction in the intensities of superstructure peaks thus showing that the ordering is being gradually lost. At 50 mol% of $Ce_{0.8}Zr_{0.2}O_2$ in $GdO_{1.5}$, i.e., the nominal composition $Ce_{0.40}Zr_{0.10}Gd_{0.50}O_{1.75}$, F-type pattern is observed. This f-type solid solution is observed in the rest of the compositions also (i.e., from $Ce_{0.48}Zr_{0.12}Gd_{0.40}O_{1.80}$ to $Ce_{0.80}Zr_{0.20}Gd_{0.00}O_{2.00}$). The lattice parameter of the F-type solid solution decreases with decrease in gadolinium content which can be attributed to the decrease in average cationic radius at cationic site. An interesting trend was observed in lattice parameters of the C-type solid solution as is reported in Table 6. Even though the average cationic radius at Gd^{3+} site decreases on doping $Ce_{0.8}Zr_{0.2}O_2$ into Gd_2O_3, the lattice parameter of the doped C-type Gd_2O_3 is higher than

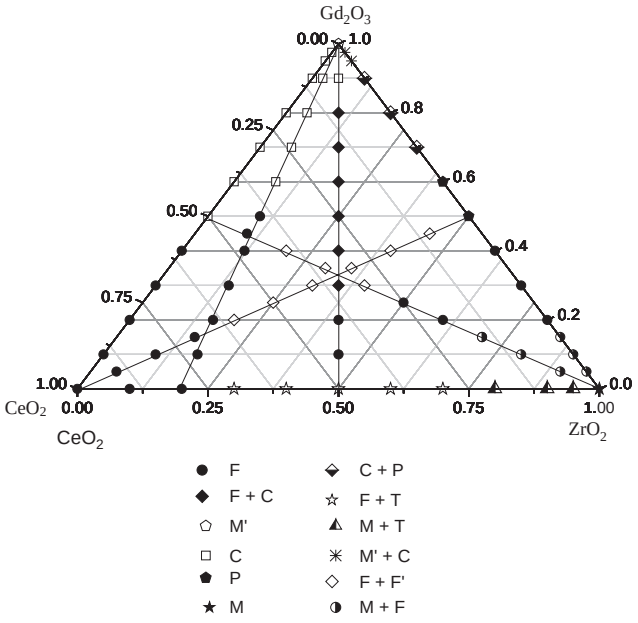

Fig. 6. Ternary phase relation in CeO_2–Gd_2O_3–ZrO_2 system.

pure Gd_2O_3. A similar trend was observed in our previous work on CeO_2–Gd_2O_3 also, as reported in the earlier section. This may be attributed to the inter-anionic repulsion between the extra anions introduced on doping tetravalent cations in gadolinia. Another plausible reason could be an increase in effective coordination number of metal ions on incorporating tetravalent cations at Gd^{3+} site.

4. Conclusions

The detailed phase relation studies in the ternary system CeO_2–ZrO_2–Gd_2O_3 (Fig. 6) revealed several interesting features. This ternary system was found to sustain a wide homogeneity range of cubic phase fields unlike that in CeO_2–ThO_2–ZrO_2 system [2]. This major difference could be attributed to that fact that unlike gadolinia, ceria is not able to stabilize cubic zirconia under the experimental conditions used by us and in turn the tetragonal zirconia was one of the major phases in CeO_2–ThO_2–ZrO_2 system. The single-phase ternary compositions, as found in this study, are expected to be superior compared to the multi-phasic compositions, for plutonium utilization. The phase equilibria in CeO_2–Gd_2O_3–ZrO_2 can be used to simulate the phase equilibria in the PuO_2–Gd_2O_3–ZrO_2 system. Some of the new single phasic compositions could also be potential electrolyte material for Solid Oxide Fuel Cells. To the best of our knowledge this is the first detailed study of phase relations in the CeO_2–Gd_2O_3–ZrO_2 system.

Acknowledgments

Authors thank Dr. N.M. Gupta, Head, Applied Chemistry Division, Bhabha Atomic Research Centre, for his keen interest and encouragement during the course of this work. Ms. A.B. Sonawane is thanked for assistance during the course of this work.

References

[1] H. Kleykamp, J. Nucl. Mater. 275 (1999) 1.
[2] V. Grover, A.K. Tyagi, J. Nucl. Mater. 305 (2002) 83.
[3] M.D. Mathews, B.R. Ambekar, A.K. Tyagi, J. Nucl. Mater. 288 (2001) 83.
[4] A.K. Tyagi, B.R. Ambekar, M.D. Mathews, J. Alloys Compds. 337 (2002) 275.
[5] G. Brauer, H. Gradinger, Z. Anrog. Allg. Chem. 276 (1954) 209.
[6] D.J.M. Bevan, E. Summerville, in: K.A. Gschneider, L. Eyring (Eds.), Handbook on the Physics and Chemistry on Rare Earths, North-Holland Publishing Company, Amsterdam, New York, Oxford, vol. 3, 1979.
[7] Z. Tianshu, P. Hing, H. Huang, J. Kilner, Solid State Ion. 148 (2002) 567.
[8] K. Heggestad, J.L. Holm, O.T. Soerensen (Lab. Electrochim.Thermdyn. Mater. Uni. Paris, Paris, Fr.) Report, RISO-M-2478, 1985, p. 23.
[9] P. Duwez, F. Odell, J. Am. Ceram. Soc. 33 (1950) 280.
[10] A. Rouanet, Rev. Int. Hautes Temp. Refract. 8 (1971) 161.
[11] H. Yahiro, Y. Eguchi, K. Eguchi, H. Arai, J. Appl. Electrochem. 18 (1988) 527.
[12] B.C.H. Steele, in: T. Takahashi (Ed.), High Conductivity Solid Ionic Conductor, Recent Trends and Applications, World Scientific, London, 1989, p. 402.
[13] V. Grover, A.K. Tyagi, Mater. Res. Bull. 39 (2004) 859.
[14] J. Wang, H. Otobe, A. Nakamura, M. Takeda, J. Solid State Chem. 176 (2003) 105.
[15] A.J. Feighry, J.T.S. Irvine, C. Zheng, J. Solid State Chem. 160 (2001) 302.
[16] C. O'driscoll, Chem. Brit. 37 (1) (2001) 16.
[17] S.X. Wang, B.D. Begg, L.M. Wang, R.C. Ewing, W.J. Weber, K.V. Govindan Kutty, J. Mater. Res. 14 (1999) 4470.
[18] K.E. Sickafus, L. Minervini, R.W. Grimes, J.A. Valdez, M. Ishimura, F. Li, K.J. McClellan, T. Hartmann, Science 289 (2000) 748.
[19] W.J. Weber, R.C. Ewing, Science 289 (2000) 2051.
[20] F. Schleifer, A. Naoumidis, H. Nickel, J. Nucl. Mater. 101 (1981) 150.
[21] G. Adachi, N. Imanaka, Chem. Rev. 98 (1998) 1479.
[22] M. Foex, J.P. Traverse, Rev. Int. Hautes Temp. Refract. 3 (1966) 429.
[23] V. Grover, S.N. Achary, A.K. Tyagi, J. Appl. Crystallogr. 36 (2003) 1082.
[24] R.D. Shannon, Acta Crystallogr. A 32 (1976) 751.
[25] S.N. Achary, S.J. Patwe, A.K. Tyagi, Mater. Res. Bull. 34 (1999) 2093.
[26] S. Meriani, G. Spinolo, Powder Diffract. 2 (1987) 255.